Solar Thermophotovoltaics: Improving the Efficiencies of Emitters and Narrow Band Gap Photovoltaic Cells

Investigators:

Shanhui Fan, Professor, Electrical Engineering, Stanford University
James Harris, Professor, Electrical Engineering, Stanford University
Mark Brongersma, Professor, Materials Science and Engineering, Stanford University

Abstract

Research in optimizing the solar cell structure used for the high efficiency solar thermophotovoltaic system was conducted during the past year. Being the final step transfering the emitted thermal radiation to electricity, it is critical to utilize high efficiency cell corresponding to the radiation spectrum, which will contribute to the total efficiency of the system. The optimization for the cell was initiated from the simulation of material selection, doping level and cell structure adjustment. We selected InGaAs to achieve narrow bandgap of 0.75eV. With proper design, we achieved cell theoretical conversion efficiency as high as 49.3 % with the total thickness of 4 μm at operation temperature of 300K. The temperature effect on the cell efficiency was further explored to provide guidance for the heat management for the final system design. The material system for cell structure simulation is also applicable to InGaAsSb and dilute nitride.

Introduction

For traditional single-junction solar cells, its efficiency is limited by the Shockley-Queisser limit. From solar spectrum, photons with energy below the band gap will not be absorbed by the cell. For photons with energy above band gap, part of the excessive energy is lost as heat. As a result, at room temperature of 300K, an ideal single junction solar cell has a theoretical maximum efficiency of 41% under solar illumination and maximum concentration. Without solar concentration, the limit is 31%.

In solar thermophotovoltaics (STPV) system, an intermediate element is heated by absorbing solar radiation. The emitted thermal radiation from the intermediary, whose spectrum can be very different from that of sunlight, is then converted into electrical energy by a solar cell. 0 shows a basic geometry. The ideal intermediary should provide broadband absorption of sunlight, as well as a narrow band emission with a wavelength tuned to the band gap of the solar cell. The maximum efficiency of the TPV cell is 85.4% when the temperature of the intermediary is maintained at $T_i = 2544K$. This efficiency is very close to the thermodynamic limit (86.8%) in any reciprocal system.

The concept of solar thermophotovoltaics[1,2,3,4,5] is appealing because it enables one to overcome the Shockley-Queisser limit with a single junction cell by utilizing nearly the entire solar spectrum. In a STPV system, one converts the sunlight into heat through a broadband absorber. The heat is then used to generate narrow-band thermal radiation from an emitter. High theoretical efficiency can be achieved if the emitter generates narrow-band radiation that is well matched in wavelength to the band gap of a single-junction solar cell (0).

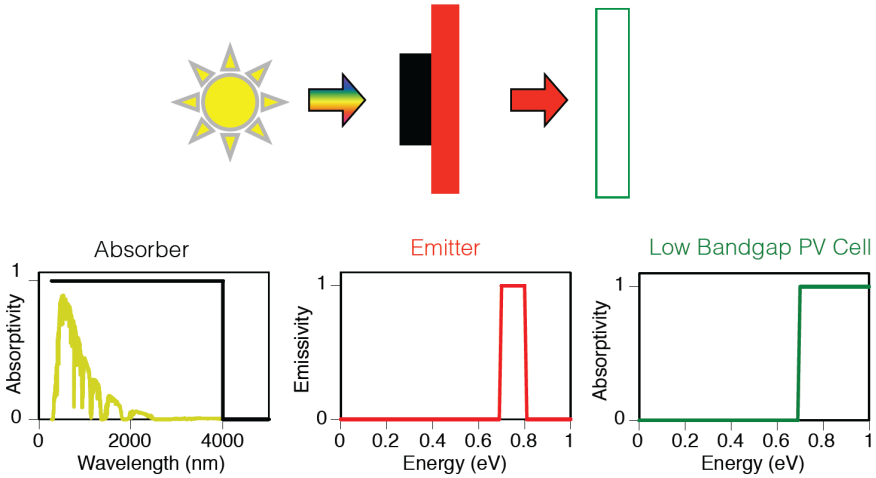

Figure 1: The concept of solar thermophotovoltaics. The black and red regions correspond to intermediate absorber and emitter, respectively. The green rectangle represents a narrow band gap cell.

Groups at MIT demonstrated a record TPV system with efficiency of 3.2%[6]. With better thermal engineering of the integrated system, they extrapolated that their system can reach efficiency in the 20% range after scaling up[Error! Bookmark not defined.]. Although this is breakthrough for TPV system research, its efficiency is still much lower than that of a single junction solar cell could provide.

Here we propose to significantly advance the fundamental science in solar TPV, by significantly improving the performance of both thermal emitters and narrow band gap solar cells. For the development of thermal emitters, we will develop novel high-temperature refractive materials, such as TiN, that exhibit strong plasmonic responses (Brongersma), and combine this with nanophotonic approach for emission control (Fan). For the developments of low band gap semiconductors solar cells, we will build upon our previous experience in demonstrating world record multi-junction cells (Harris), to develop narrow band gap material systems and combine these material systems with nanophotonic approach for efficiency.

Background

One of the biggest efficiency limiting factor for the whole TPV system is the narrow band gap TPV cell, which requires the accurate match of the cell bandgap and the emitter spectrum, good material quality and low cell operating temperature. The InGaAs single junction cell lattice-matched to InP substrate can be good candidate for a TPV system. InGaAs cell in this study has a band gap of 0.75 eV and a composition as $In_{0.53}Ga_{0.47}As$.

In this case, a systematical simulation of $In_{0.53}Ga_{0.47}As$ TPV cell was conducted using Rsoft Lasermod under certain thermal emission spectrum from the thermal emitter. The tailored emitter spectrum with the peak energy aligned to the band gap of the $In_{0.53}Ga_{0.47}As$ was first calculated and used as the incident light spectrum. The cell performance was simulated with the variation of (a) the window/back surface field (BSF) layer doping, (b) the emitter/base thickness and (c) the cell temperature. The original cell epitaxial design is based on the structure reported in [8]. In the optimization process, the cell temperature was first set at 300 K, the doping levels of the window and BSF were adjusted. In the next step, the thicknesses of the emitter and base layer were varied

respectively to obtain an optimized V_{OC} and cell efficiency. With the optimized structure at temperature of 300 K, the temperature effect on the cell efficiency was further analyzed and discussed. Our simulation results showed that the $In_{0.53}Ga_{0.47}As$ cell is able to reach conversion efficiency of 49% at 300 K. However, as temperature increases to 500 K, the simulated efficiency drops to 33%.

Results

Thermal Emitter Design

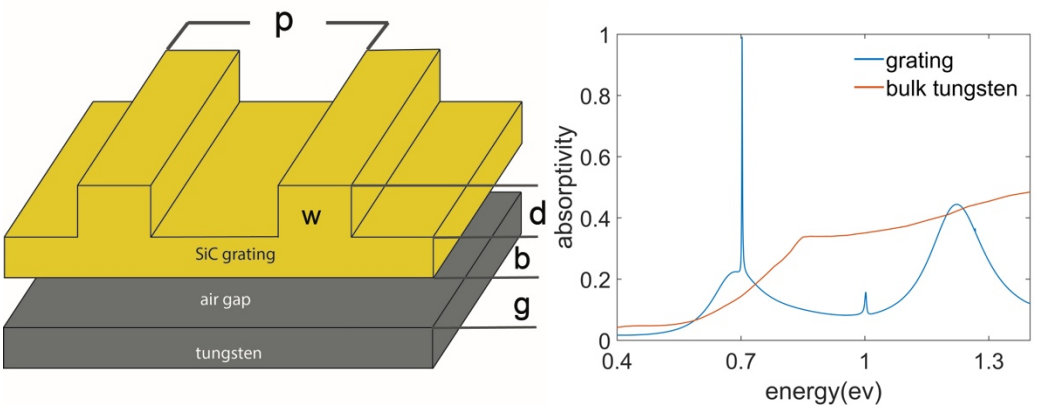

Figure 2: (a) (left) Schematic of the emitter design. (b) (right) Narrowband thermal emission peaking at 0.7eV.

Tungsten is a widely used high temperature material due to its high melting point and low vapor pressure. Thus we choose tungsten as the thermal emitter. However, bulk tungsten has low emissivity in the near-IR region, which necessitates optical engineering to tailor its emissivity.

We use critical coupling between the guided resonances of photonic crystal (PhC) slab and tungsten to achieve perfect absorption and thus hundred percent emissivity. Critical coupling occurs when intrinsic loss equals external loss. In our case the absorption in tungsten slab is the intrinsic loss of the resonances, and the coupling of the guided modes to free space radiation is the external loss. Since the guided modes decay fast away from the photonic crystal slab due to their evanescent nature, the intrinsic loss decreases as the air gap size between photonic crystal slab and tungsten increases. This enables us to tune through critical coupling by adjusting the gap size.

Here we take silicon carbide (SiC) as the dielectric of the PhC slab, which has an optical constant of about 6.6 in the frequency region of interest. We consider a 1D grating as shown in Fig. 4(a). The grating width (w) is fixed to be half of the periodicity; the effective thickness of the slab (b+d/2) is fixed to be 0.4um for PhC slabs. The choices of moderate dielectric constant and slab thickness ensure a low emissivity background in the absence of any patterning, in addition to providing guided modes. Unless otherwise specified, the incident wave is s-polarized coming in the normal direction.

To achieve a guided resonance at 0.7eV, the periodicity of the 1D grating is found to be 0.81um. We choose a grating depth of 0.02um, and scan the gap size to find that its value at critical coupling is 0.18um. In Fig. 4(b), we show the absorption spectrum of tungsten at critical coupling

and also that of bulk tungsten. We find a distinct peak at the target 0.7eV, and no resonances existing at lower frequencies. Note that with the photonic crystal slab, the absorption can be suppressed in a broad frequency range (0.8eV to 1.4eV) off the main resonance, which is advantageous for energy efficiency. We can also vary the periodicity and the grating depth to achieve perfect emissivity at other frequencies with various linewidth.

Cell Simulations

1. $In_{0.53}Ga_{0.47}As$ cell structure and emission spectrum

The $In_{0.53}Ga_{0.47}As$ cell structure, as illustrated in Fig 2, was designed based on the similar design previous reported in [8]. The doping concentration and thickness of each layer are listed in Table I.

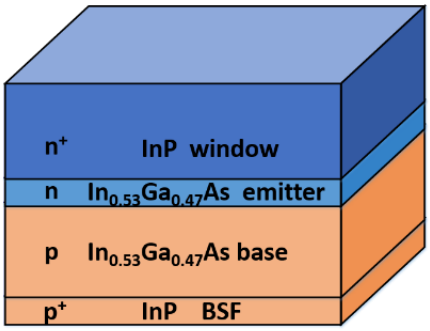

Figure 3. Schematic of the structure of the simulated $In_{0.53}Ga_{0.47}As$ cell

The 0.75 eV band gap $In_{0.53}Ga_{0.47}As$ cell is lattice matched to InP substrate.

TABLE I
ORIGIN THICKNESS AND DOPING CONCENTRATION

	Window (n-type)	Emitter (n-type)	Base (p-type)	BSF (p-type)
Thickness (μm)	1.5	0.2	2.5	0.3
Doping (cm^{-3})	1×10^{18}	1×10^{18}	1×10^{18}	1×10^{18}

In a TPV system, the incident light collected by the cell is a tailored narrow band width spectrum from the emitter's blackbody irradiation. In our study, to get the highest efficiency, the incident spectrum was tailored to match the absorption of the $In_{0.53}Ga_{0.47}As$ cell. The band gap (E_g) of the $In_{0.53}Ga_{0.47}As$ cell corresponds to the wavelength (λ) of 1.65 μm calculated with the relationship of $E_G = \frac{hc}{\lambda}$, where h is the Planck constant, c is the light speed. The relationship between the peak of the emission spectrum and the temperature follows the equation:

$$\lambda_{peak} = \frac{b}{T} \qquad (1)$$

where the constant b is Wien's displacement constant, which is equals to 2.898×10^{-3} K m. λ_{peak} is the wavelength of peak of the spectrum, and T is the temperature. Substituting the wavelength corresponding to the bandgap of the InGaAs (0.75 eV), the corresponding temperature is T=1751 K. The black body irradiance was calculated based on the Planck's Law:

$$I(\lambda, T) = \frac{2hc^2}{\lambda^5} \frac{1}{e^{\frac{hc}{\lambda kT}} - 1} \quad (2)$$

where $I(\lambda, T)$ is the blackbody irradiance, k is the Boltzmann constant, T is the temperature. The calculated spectrum is shown in Fig 3. Noted that in order to conduct the simulation, the irradiance was taken the solid angle as 1 sr. The incident light was selected with the wavelength range from 1.47 μm to 1.65 μm (corresponding to the band gap of 0.85 eV and 0.75 eV).

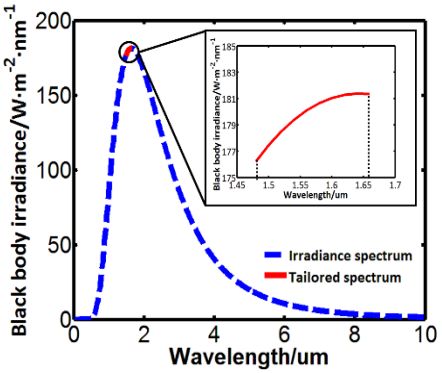

Figure 4. Calculated blackbody irradiance spectrum

2. Window and BSF layer doping level

First, doping concentration of the Window layer and BSF layer was changed to value of 1×10^{18} cm^{-3}, 1×10^{19} cm^{-3} and 1×10^{20} cm^{-3} respectively. The J-V curves were simulated and are shown in Fig 4 and the detailed simulation result was shown in Table II.

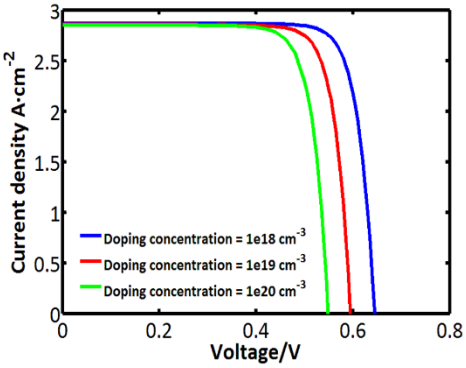

Figure 5. Simulation results of the InGaAs cell with different Window & BSF doping concentrations.

The short circuit current J_{sc} remains relatively constant while the open circuit voltage V_{oc} decreases from 0.65 V to 0.55 V as the doping level increases from 1×10^{18} cm^{-3} to 1×10^{20} cm^{-3}, indicating more recombination in the Window and BSF layer due to higher doping level. Such effect decreases the cell efficiency from 43.1% to 35.5%.

TABLE II
SIMULATION RESULTS WITH DOPING LEVEL

Doping/cm^{-3}	1×10^{18}	1×10^{19}	1×10^{20}
Efficiency /%	43.1	39.3	35.5

$J_{sc}\,/A\cdot cm^{-2}$	2.87	2.86	2.85
$V_{oc}\,/V$	0.650	0.600	0.550
FF /%	82.1	81.3	79.9

With the optimized window and BSF doping level of 1×10^{18} cm^{-3}, the thickness of the emitter layer was changed to values of 0.1 μm, 0.2 μm and 0.5 μm. The simulation result is shown in Fig 5 with details shown in Table III.

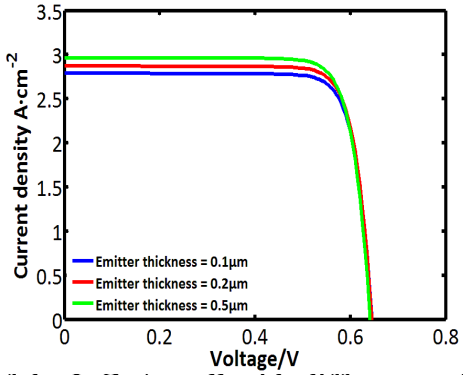

Figure 6. Simulation results of the InGaAs cell with different emitter thicknesses of 0.1 μm, 0.2 μm, 0.5 μm.

TABLE III
SIMULATION RESULTS WITH EMITTER THICKNESS

Thickness/μm	0.1	0.2	0.5
Efficiency /%	41.9	43.1	44.0
$J_{sc}\,/A\cdot cm^{-2}$	2.79	2.86	2.96
$V_{oc}\,/V$	0.650	0.650	0.650
FF / %	81.1	82.1	81.4

The V_{oc} remains relatively the same at 0.65 V, with a slight increase of J_{sc} from 2.79 A/cm^2 to 2.96 A/cm^2, indicating addition light absorption in the thicker Emitter layer, which leads to the increase of cell efficiency from 41.92% to 44.04%.

The thickness of the base layer was further optimized with the values of 0.5 μm, 2.5 μm and 3.5 μm. The result is shown in Fig 6 with the details in Table IV.

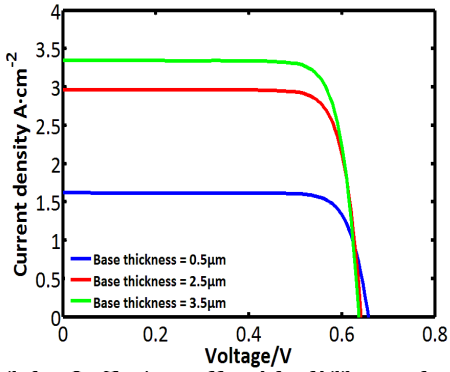

Figure 7. Simulation results of the InGaAs cell with different base thickness of 0.5 μm, 2.5 μm, 3.5 μm.

TABLE IV
SIMULATION RESULTS WITH EMITTER THICKNESS

Thickness/μm	0.5	2.5	3. 5
Efficiency /%	24.7	44.0	49.3
$J_{sc}/A \cdot cm^{-2}$	1.62	2.96	3.34
V_{oc}/V	0.660	0.650	0.640
FF / %	81.6	82.1	81.4

While the V_{oc} slightly decreases from 0.65 V to 0.64 V, the J_{sc} doubles from 1.62 A/cm^2 to 3.34 A/cm^2, which leads to a significant increase in the efficiency from 24.7% to 49.3%. Such efficiency also reaches the best simulation result, with the parameters listed in Table V.

TABLE V
OPTIMIZED PARAMETERS OF THE CELL

	Doping /cm^{-3}	Emitter /μm	Base /μm	Efficiency /%
Value	1×10^{18}	0.5	3.5	49.3

3. Temperature effect

Since the emitter in the TPV system would be at a high temperature (1751 K in this study), it is important to evaluate the cell performance at temperatures higher than 300 K. The temperature effect on the $In_{0.53}Ga_{0.47}As$ cell was further explored, with the result shown in Fig 7. The details were shown in Table VI.

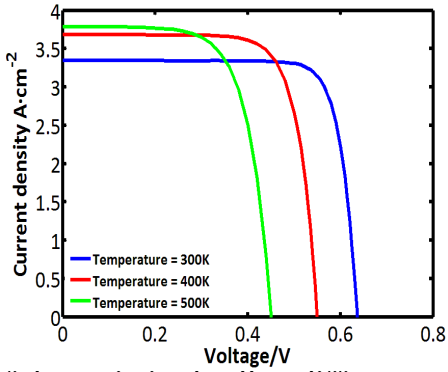

Figure 6. Simulation results of the optimized cell at different cell temperature of 300 K, 400 K, 500 K.

TABLE VI
SIMULATION RESULTS WITH TEMPERATURE

Temperature/K	300	400	500
Efficiency /%	49.3	43.7	33.4
$J_{sc}/A \cdot cm^{-2}$	3.34	3.68	3.79
V_{oc}/V	0.64	0.55	0.46
FF / %	81.4	76.0	67.6

The higher temperature results in a slightly higher J_{sc}, but the corresponding V_{oc} drops rapidly

resulting in the decrease of the cell efficiency from 49.3% to 33.4%. The result shows the importance of heat management to maintain the low cell operating temperature in the TPV system.

Publications

1. Y. Guo and S. Fan, "Narrowband thermal emission from a uniform tungsten surface critically coupled with a photonic crystal guided resonance", Optics Express, vol. 24, pp. 29896-29907 (2016).

2. V. Fernandez-Hurtado, F. J. Garcia-Vidal, S. Fan, and J. C. Cuevas, "Enhancing near-field radiative heat transfer with Si-based metasurfaces", Physical Review Letters, vol. 118, art. No. 203901 (2017).

Reference

[1] R. M. Swanson, "A proposed thermophotovoltaic solar energy conversion", Proceedings of IEEE 67, 446 (1979).

[2] N. -P. Harder, P. Wurfel, "Theoretical limits of thermophotovoltaic solar energy conversion", Semiconductor Science and Technology 18, S151 (2003).

[3] S. Fan, "An altenative sun for solar cells", Nature Nanotechnology 9, 92-93 (2014).

[4] A. Narayanaswamy and G. Chen, "Surface modes for near field thermophotovoltaics", Applied Physics Letters 82, 3544 (2003).

[5] A. Datas and C. Algora, "Development and experimental evaluation of a complete solar thermophotovoltaic system", Progress in Photovoltaics: Research and Applications 21, 1025 (2012).

[6] A. Lenert, D.M. Bierman, Y. Nam, W.R. Chan, I. Celanovic, M. Soljacic, E.N. Wang, "A nanophotonic solar thermophotovoltaic device", Nature Nanotechnology, 9, 126 (2014).

[7] K. A. Arpin, M. Losego, A. N. Cloud, H. Ning, J. Mallek, N. P. Sergeant, L. Zhu, Z. Yu, B. Kalanyan, G. N. Parsons, G. S. Girolami, J. R. Abelson, S. Fan, and P. V. Braun, "3D self-assembled photonic crystals with high temperature stability for thermal emission modifications", Nature Communications 4, 2630 (2013).

Contacts

Shanhui Fan: shanhui@stanford.edu
James Harris: jharris@stanford.edu
Mark Brongersma: markb29@stanford.edu